

Occurrence of hydrothermal kaolin minerals beneath the Iheya North Knoll hydrothermal field in the Okinawa Trough

TSUTSUMI, Saki^{1*}; ISHIBASHI, Jun-ichiro¹; UEHARA, Seiichiro¹; SHIMADA, Kazuhiko¹; MIYOSHI, Youko²; NOZAKI, Tatsuo³; TAKAYA, Yutaro³

¹Department of Earth and Planetary Sciences, Graduate School of Sciences, 33 Kyushu University, ²National Institute of Advanced Industrial Science and Technology, ³Japan Agency for Marine-Earth Science and Technology

Introduction

Kaolin minerals is known as common alteration minerals observed in on land geothermal or fumarole area. On the other hand, only few studies reported occurrence of kaolin minerals in seafloor hydrothermal fields. As an example, occurrence of kaolin minerals was reported at the Jade site in the Izena Hole in the Okinawa Trough by Marumo and Hattori (1999). Recently, seafloor drillings conducted at the Iheya North Knoll in the Okinawa Trough revealed occurrence of kaolin minerals in sediment cores obtained from the vicinity of active hydrothermal fields. We conducted X-ray diffractometric analysis (XRD) and Scanning Electron Microscope (SEM) observation of the sediment samples. In this presentation, we report depth profiles of clay mineral assemblage in sediment below active hydrothermal fields, with interest in the relationship with a profile of metal elements content in the sediment.

Sampling and methods

Sediment cores were obtained by drilling at Hole C9016B (27° 46.6' N, 126° 54.6' E, depth = 1124m) in the vicinity of Aki site during CK-14 expedition in 2014, and by drilling at Site BMS-I-4 (27° 47.4' N, 126° 53.9' E, depth = 1048m) located 200 m east from the Original site, during TAIGA11 cruises in 2011. Identification of clay minerals was conducted by X-ray diffraction technique (XRD) after separation of clay minerals and by scanning electron microscope (SEM) observation of bulk sediment.

Results and discussion

In the Aki site, change of dominant clay mineral assemblage along depth was recognized as below; smectite and illite in 0-9 mbsf, illite and kaolin mineral in 9-11 mbsf, and illite and Mg-chlorite below 11 mbsf (to 91 mbsf). Detailed investigation of the kaolin-rich layer revealed change of occurrence of kaolin minerals along depth as below; spherical kaolin minerals at 8.88 mbsf, plate-like kaolinite and tubular halloysite at 9.18 mbsf, and crystal kaolin minerals at 10.83 mbsf. It is interesting to note occurrence of sphalerite and barite were identified in the 9.18 mbsf sediment but not observed in 10.84 mbsf. Profile of trace elements content in bulk sediment (Nozaki et al., in this meeting) corresponded to the occurrence of sulfide/sulfate minerals in the sediment. High contents of Ba, Zn and Pb were notable in the 9.81 mbsf sediment, whereas high contents of Cu and Ag were recognized in the 10.28 mbsf sediment.

In the Original site, intense alteration represented by dominant occurrence of kaolin minerals was recognized in sediment from just a few 10 cmbsf to 3.5 mbsf. Also in the sediment from this site, occurrence of sphalerite, galena and barite was identified.

As mentioned above, occurrence of kaolin minerals associated with sphalerite and barite was recognized in relatively shallow depth below the seafloor located at a few hundred meters apart from the active venting in two hydrothermal sites in the Okinawa Trough.

Keywords: submarine hydrothermal deposit, clay minerals, submarine drilling

The structure of iron oxidized mounds at shallow marine hydrothermal environment in Satsuma Iwo-jima Island, Kagoshima

KURATOMI, Takashi^{1*}; KIYOKAWA, Shoichi¹; IKEHARA, Minoru²; GOTO, Shusaku³; HOSHINO, Tatsuhiko⁴; IKEGAMI, Fumihiko¹; MINOWA, Yuto¹

¹Kyushu University, ²Center for Advanced Marine Core Research, Kochi University, ³Geological Survey of Japan, AIST, ⁴Japan Agency for Marine-Earth Science and Technology

Satsuma Iwo-Jima, located 38km south of Kyusyu Island, Japan, is a volcanic island in the northwestern rim of Kikai caldera. Here is preserved and identified on occurring iron precipitation at shallow ocean where can be recorded modern analogy of iron precipitation and sedimentation. Iron oxidized mounds are developing at seafloor with hydrothermal activity (pH=5.5, 50-60 degree Celsius), and there is high deposition rate of iron-oxides (33 cm/year: Kiyokawa et al., 2012).

Result of sea sonar scan seismic images shows that the iron oxidized mounds in Nagahama bay are estimated about 7.8 m³ in volume, which formed 2-3 thick mound at 32.68 m² area for 20 years. Each mound is formed two layers: blackish hard layer and brownish soft layer. The inside of samples is constructed from the aggregation of convex structure (3-4 cm) covered by hard layers as a rim. Petrographic observations indicate that both layers have filament-like forms, and the form in soft layer is perpendicular to that in the hard layer. The number of iron oxides particles observed on filament-like forms in soft layer increases toward hard layer. Hard layer consists of aggregation of bacillus-like form as the chain of particle (about 2 um). At soft layer, on the other hand, bacteria-like form with smaller particles (<0.5 um) is observed. Bacteria-like form could be classified into 3 types (helix, ribbon-like, twisted). Furthermore, hard layers consist of ferrihydrite and opal-A (Si: 26.8%, Fe: 56.0%) and soft one is composed by ferrihydrite, opal-A and silica mineral (Si: 36.5%, Fe: 43.5%). *Mariprofundus ferrooxydans* known as iron-oxidizing bacteria belonging to Zeta-proteobacteria identified in this matter, but they are nothing at floating iron oxide samples.

The process of forming iron oxidized mounds: 1. Soft layers were made by chemical and biological activity. The filament-like forms at soft layer is the stalks of iron oxidizing bacteria. 2. The hard layers were made by adsorption of iron oxyhydroxide around stalks. Iron oxidizing bacteria is prefer to the redox interface (Chan et al., 2011) such as the mixing zone located in hard layer between hydrothermal fluid and seawater. 3. Hydrothermal activity form the liner structure at hard layer. Iron oxidized mounds were formed by repeating of those process over ten times.

Based on the seismic data, the forming rate of iron oxidized mounds is about over 1.2 cm/yr. Formation of hard layers in these mound is the result of adsorption of iron oxyhydroxide around stalks made by the activity of iron oxidizing bacteria. The iron providing rate (2.474×10^6 kg(Fe)/m.y./m²) from the Nagahama bay iron mounds is as about ten times as that of the Hamasley Group sediment (2.51×10^5 kg(Fe)/m.y./m²). Furthermore, if there is the Nagahama bay iron oxidized mounds at Archean, 6.0×10^8 times of these mounds need to form the Joffre Member volume (360 m/2m.y.). In this study, we strongly suggest that the combination of chemical and biological reaction is important system to form large amount of iron oxide deposit.

Keywords: iron oxidizing bacteria, hydrothermal fluid, iron oxide, satsuma iwo jima, biomineralization

Geochemistry of trace alkali elements in the seafloor hydrothermal fluids

EBINA, Naoya^{1*}; ISHIBASHI, Jun-ichiro²

¹Department of Earth and Planetary Sciences, Graduate School of Sciences, Kyushu University, ²Department of Earth and Planetary Sciences, Faculty of Science, Kyushu University

Hydrothermal fluid contains many elements at high concentrations as a result of fluid interaction with rock/sediment and seawater during fluid circulation beneath the seafloor. In particular, Rb and Cs are known as "soluble elements" which is easily leached from the rock/sediment into the fluid because of their large ion radii. Thus, trace alkali element compositions of hydrothermal fluids would provide information about water/rock interactions.

We determined Rb and Cs concentrations of hydrothermal fluids collected from four fields in the Izu-Ogasawara arc (Myojin Knoll Caldera, Myojinsho Caldera, Bayonnaise Knoll Caldera and Suiyo Seamount), from six fields in the Mariana Trough (Alice Springs Field, Forecast Vent Field, Pika Site, Archean Site, Snail Site and Urashima Site), and from the Iheya North Knoll hydrothermal field in the Okinawa Trough, to discuss their diversity.

Analysis of Rb and Cs concentrations of each sample was conducted using ICP-QMS. To determine the endmember Rb and Cs compositions for each hydrothermal field, the analytical results of the samples were extrapolated to zero Mg concentration. The endmember concentrations of Rb and Cs are plotted in Figure 1. In addition to the results of this study, data from hydrothermal field in the EPR 21°N^[1] and MAR (TAG and MARK)^[6] located in sediment-starved mid ocean ridge setting, in the Escanaba Trough and Guaymas Basin^[2] located in a sediment-hosted setting, and in the Lau Basin^[3] and Manus Basin^[4] located in a back-arc basin setting are plotted in the same figure. Moreover, compiled data for volcanic rocks and sediment material around these hydrothermal field are overimposed as shaded region in Figure 1.

A range of Rb/Cs ratio of hydrothermal fluids from an arc setting (square symbols; Rb/Cs=12.8 to 26.7) can be distinctive that from a back-arc basin setting (circle symbols; Rb/Cs=18.6 to 100.1). Rb and Cs concentrations in hydrothermal fluids from a sediment-hosted hydrothermal field is characterized by their substantially high concentrations. Moreover, it is likely that the range of Rb/Cs ratio of hydrothermal fluids are comparable for those of volcanic rocks/sediment surrounding these hydrothermal field. It would be suggest that the distribution of Cs from rocks to hydrothermal fluids in arc setting is higher than one in other tectonic setting.

[1] Palmer and Edmond (1989) *Earth and Plan. Sci. Let.*, **95**, 8-14.

[2] Campbell et al. (1994) *U.S. Geol. Surv. Bull.*, No. **2022**, 201-221.

[3] Mottl et al. (2011) *Geochimica et Cosmochimica Acta*, **75**, 1013-1038.

[4] Reeves et al. (2011) *Geochimica et Cosmochimica Acta*, **75**, 1088-1123.

[5] de Ronde et al. (2011) *Miner Deposita*, **46**, 541-584.

[6] Campbell et al. (1988) *Nature*, **335**, 514-519.

Keywords: trace alkali elements, hydrothermal fluids, arc, back-arc basin, sediment

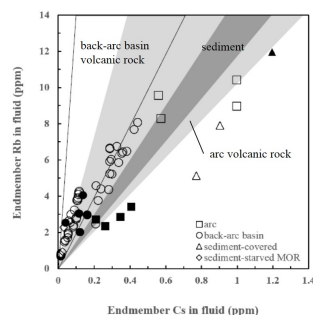


Fig. 1 Relationship between Rb and Cs end-member concentrations in hydrothermal fluids measured this study (solid symbols) and compiled data from sedimentary hydrothermal systems of various tectonic setting (open symbols). Symbols are: squares, Izu-Ogasawara and Kermadec arc^[1] of arc hydrothermal systems, circles, mid-southern Mariana Trough, Lau Basin^[2] and Manus Basin^[4] of back-arc basin (BAB) hydrothermal systems, triangles: Iheya North Knoll at Mid Okinawa Trough, Guaymas Basin and Escanaba Trough^[5] of sediment-hosted hydrothermal systems, and diamonds: EPR 21°N^[1], TAG and MARK^[6] in Mid Atlantic Ridge of sediment-starved mid-ocean ridge (MOR) hydrothermal systems. Moreover, the range of Rb/Cs in volcanic rock collected around each hydrothermal site were compiled and were drawn meshing in Fig. 1. The meshing show: area surrounded solid line: BAB volcanic rock, dark grey: sediment, and light grey: arc volcanic rock, respectively.

Seismicity at the Kairei Hydrothermal Vent Field Near the Rodriguez Triple Junction in the Indian Ocean

MORI, Taiyu^{1*} ; SATO, Toshinori¹ ; TAKATA, Hiroyoshi¹ ; IMAI, Yuki¹ ; NOGUCHI, Yui¹ ; KONO, Akihiro¹ ; YAMADA, Tomoaki² ; SHINOHARA, Masanao²

¹Chiba Univ., ²ERI, Univ. Tokyo

1. Introduction

In the first segment of the central Indian Ridge from the Rodriguez triple junction, the Kairei hydrothermal vent field exists and extrudes hydrothermal fluid with richer hydrogen content compared to other hydrothermal vents in the world. Around the Kairei hydrothermal field, serpentinized peridotite and troctolites, and gabbroic rocks were discovered. These deep-seated rocks exposed around the Kairei field may cause the enrichment of H₂ in the Kairei fluids. At the Kairei field, a hydrogen-based subsurface microbial ecosystem and various hydrothermal vent macrofauna were found. In the "TAIGA" Project (Trans-crustal Advection and In situ reaction of Global sub-seafloor Aquifer), this area is a representative field of "TAIGA" of hydrogen. To investigate how the deep-seated rocks (originally situated at several kilometers below seafloor) are uplifted and exposed onto seafloor, and the hydrothermal fluids circulate in subsurface, we conducted a seismic refraction/reflection survey and seismicity observation with ocean bottom seismometers (OBSs). This presentation will show seismicity of the survey area.

2. Observation and methods

We conducted a seismic survey around the Kairei hydrothermal field from January 27 to March 19 in 2013 using S/V Yokosuka of Jamstec (YK13-01, YK13-03). We used 21 OBSs. We determined hypocenter locations in a 3D velocity structure. The 3D structure is estimated by Takata et al. (2015, This Meeting). We used NonLinLoc software (Lomax, 2000), which can estimate earthquake locations in 3D media.

3. Results

From the 50 days seismicity observation, we found more than 5000 micro earthquakes in this area. A swarm of micro earthquakes exists at a location about 1-3 km northwest of the Kairei field. The swarm has a NNW-SSE strike, parallel to the ridge axis. The depth of the swarm is very shallow (~4 km from seafloor). The focal mechanisms in the swarm are normal type. These indicate that this swarm shows normal fault activity parallel to the ridge axis. This swarm may be related to the hydrothermal activities of the Kairei field. At the first segment of the central Indian Ridge, many micro earthquakes occurred. The depth of these events is about 3-6 km from seafloor, and deeper than that of the swarm near the Kairei field. The focal mechanisms at the segment are normal type with the T axis parallel to the plate motion. At the non transform offset, there are no lineaments of earthquakes and left lateral strike slip mechanisms are dominant.

Acknowledgements

We thank the captain and the crew of S/V Yokosuka of Jamstec for their support. This work was supported by Grant-in-Aid for Scientific Research on Innovative Areas of the Ministry of Education, Culture, Sports, Science and Technology (Grant Number 20109002, TAIGA project).

Keywords: TAIGA Project, hydrothermal field, seismicity, Triple Junction in the Indian Ocean

Petrographical and morphological character of volcanic rocks dredged around the Sumisu caldera, Izu-Ogasawara arc

UEHARA, Taiki^{1*} ; SAKAMOTO, Izumi¹ ; YAGI, Masatoshi¹ ; INOUE, Tomohito¹ ; OKAMURA, Satoshi²

¹School of marine science and technology, ²Hokkaido Education University, Sapporo Campus

The Izu-Ogasawara arc is located the south of Izu peninsula. It opens for total extension approximately 1,500km, approximately 400km in width. In addition, it is an active oceanic island arc of the volcanic activity. A volcanic zone of the Quaternary period ranges to the Shititou-Ioushima ridge in the Izu-Ogasawara arc to the north and south and constitutes a volcanic front. There are many submarine volcano with caldera in the Izu-Ogasawara arc (Murakami, 1997).

In this study, mention of the topography of Smith caldera gathered by Tokai University Bousheimaru from May 9, 2014 through May 15 and the rock analyzed it.

As a result, (1)the diameter of the Sumisu caldera is 9km (2)the depth of the water of the outer rim of a volcanic crater top is 30m (3)caldera wall is steep than the outer slope (4)stepped terrain development in the caldera outside slope (5)water depth of caldera bottom 900m (6)there exists a central cone of relative height 100m in the center. As a result of bottom sampling, fresh rhyolite volcanic rock and volcano-clastic rock were gathered from a caldera bottom and the central cone. Fresh rhyolite volcanic rock rhyolite was gathered in the lower caldera wall and central part. By the petrochemistry composition, a value of SiO₂ was concentrated in two places of 49.6(wt.%)~51.1(wt.%) and 67.5(wt.%)~69.4(wt.%). Typical bimodal volcanic activity was confirmed from this caldera.

From the slope of the back arc side, flat basalt and a large quantity of pumice and acid plutonic rocks were collected. A large quantity of dacite quality pumice (quality of corner stone) was gathered at the same time, too. Therefore, bimodal volcanic activity was estimated in the back arc side than not including volcanic rock of the quality of andesite.

Keywords: Smith caldera, Bimodal volcanism, Spatter ejecta, Dacitic pumice

Petrological study on Marcus Island

KAWANO, Takaomi^{1*} ; HIRANO, Naoto² ; MORISHITA, Taisei³

¹Graduate School of Science and Faculty of Science, Tohoku University, ²Center for Northeast Asian Studies, Tohoku University,

³Hydrographic and Oceanographic Department, Japan Coast Guard

Marcus-Wake seamount trail is located in West Pacific Seamount Province (WPSP), where the oceanic plate is oldest in the world, around 160 Ma Pacific plate. WPSP had occurred during Cretaceous and was reconciled with current active hotspots of French Polynesia in South Pacific. Marcus (Minami-tori) Island is located 50 km away from Marcus-Wake seamount trail to the north. Most of seamounts, particularly well-studied seamounts, are more voluminous than the edifice of Marcus Island, whereas no islands and atolls are found around the island within 500 km. In this study, mineralogical and whole rock analysis of lava samples, obtained in submarine survey of northwest flank of Marcus Island, are adopted in order to compare with volcanic samples from WPSP and South Pacific islands of active hotspot volcanism. High TiO_2 in relic of chrome spinel indicates the typical intra-plate volcanism to be similar characteristics with those of WPSP. Major element compositions reveal normal-alkali basalts. Nb/Zr and Nb/Y ratios can classify the origins of shallow mantle plume, not in superplume as old Polynesian hotspots, like the Marcus-Wake seamounts of WPSP. Therefore, Marcus Island was produced from intraplate volcanism which differs from hotspot activities forming the Marcus-Wake seamounts.

Keywords: Marcus-Wake seamount trails, seamount, WPSP, HFSE, superplume, alkali-basalt

Olivine xenocrysts in lava of petit-spot volcano

TAKI, Arashi^{1*} ; HIRANO, Naoto² ; YAMAMOTO, Junji³ ; MACHIDA, Shiki⁴ ; ISHII, Teruaki⁵

¹Graduate School of Science, Tohoku University, ²Center for Northeast Asian Studies, Tohoku University, ³Hokkaido University Museum, ⁴Department of Resources and Environmental Engineering, Waseda University, ⁵Fukuda Geological Institute

Petit-spot is a small volcano erupted on the seafloor. The magma comes from asthenosphere, just below oceanic lithosphere, through a crack in subducting plate. The petit-spot volcanoes appear globally on the seafloor where the plate is flexing (e.g., Japan and Chile Trenches). The petit-spot lavas and entrained mantle materials have been already reported from areas of Japan Trench oceanward slope (Sites A), and of NW Pacific (Site B). Although the discovery of the petit-spots has been anticipated from Site C (offshore of Fukushima, south of Site A), lava samples and entrained mantle materials have never been reported. To examine the activity of the petit-spot volcanoes, we conducted the nine submersible dives of the *SHINKAI 6500* submersible during cruise YK14-05 of *R/V Yokosuka* at Site C in April 2014.

Alkaline pillow lavas were collected from the Site C during cruise YK14-05. Eruption age is at the time between 0.31 and 2.1 Ma estimated on the basis of the thickness of paragonite on quenched glass rind. The lavas are classified into basanite, and include large amount of olivine (>10% normative olivine). Large (1-5 mm) olivines have anhedral morphology. The large olivines show forsterite numbers (Fo) of 88-90 and NiO contents of 0.3-0.5 wt. %, corresponding to the composition of the primitive mantle peridotite. On the other hand, the small olivines surrounding the large olivines have similar range of compositions (Fo of 84-87, CaO contents of >0.1 wt. %) to those of groundmass olivines. These observations imply that large olivines are fragments of mantle peridotites, that is, these are mantle xenocrysts. If these are xenocrystic olivines, it tells us the cryptic aspects of an old oceanic lithosphere. Fo values of the present olivine xenocrysts are slightly lower than those of the mantle xenoliths reported from Site A and B (90-93). The chemically heterogeneous mantle might be existed in the subducting NW Pacific plate.

Keywords: petit-spot, olivine, xenocryst

Petrological analysis of Fe(III)-rich serpentine in the Central Indian Ridge serpentinites

SHIMIZU, Shota^{1*}; MIZUKAMI, Tomoyuki¹; SODA, Yusuke¹; MORISHITA, Tomoaki¹; ARAI, Shoji¹; TAKAHASHI, Yoshio²

¹School of Natural System, College of Science and Engineering, Kanazawa University, ²Department of Earth and Planetary Science, Graduate School of Science, The University of Tokyo

Aqueous fluids at serpentinite-hosted hydrothermal vent fields near mid-oceanic ridges are characterized by high concentrations of dissolved reducing chemical species, such as H₂, H₂S and hydrocarbons, and aid development of unusual chemosynthetic ecosystems. Petrological, geochemical and experimental works suggest that the cause of the H₂-rich fluids is oxidation of Fe during water-rock reactions in ultramafic lithosphere to form magnetite. However, a recent micro-XANES study of the Mid-Atlantic Ridge serpentinite indicates that serpentine can be a primary phase for Fe³⁺ prior to magnetite. In order to understand the role of Fe³⁺-rich serpentine in the H₂ production, we made petrological analyses of serpentinite exposed at the southern end of the Central Indian Ridge (CIR), very close to the Kairei Hydrothermal Field where high temperature, H₂- and Si-rich fluids are emitting. Serpentine samples used in this study (dredged using Hakuho-maru from Yokoniwa Rise) include 11-13 modal % of bastite after Opx indicating that the protoliths are mantle peridotite with harzburgite compositions.

Base on microscopic observations and micro-Raman and EPMA analyses, we identified three types of serpentine after olivine. The most dominant one is characteristically brownish under microscope and optically isotropic. The Raman O-H bands are distinct from those of typical serpentine polymorphs but can be explained as composites of chrysotile and lizardite. Therefore, we call this type of occurrence as “brown serpentine aggregate”. It occupies about 70 vol % of the samples. Extensive replacement of olivine by brown serpentine (Stage I) was followed by formation of Fe-rich lizardite along pre-existing magnetite (Stage II), resulting in a mesh-like texture. During a later stage of hydrothermal alteration (Stage III), the mesh texture has been partly or fully overprinted by a vein-like texture consisting of Fe-poor well-crystalline lizardite and crack-filling chrysotile at its center. The microtextural evolution represents stepwise serpentinization probably during uplifting of the CIR mantle lithosphere.

Distribution and mineral chemistry of “brown serpentine” indicate that SiO₂ activity was a significant driving force of the formation. Total oxide compositions of “brown serpentine” are significantly lower than that of lizardite implying fine-grained aggregates with porous nature. They can be interpreted as a product of high reaction rate under high temperature conditions.

Preliminary micro-XANES analyses of “brown serpentine” at a mesh center revealed that about 70% of Fe in the serpentine is Fe³⁺. Assuming that this value is applicable to the whole sample and that the bulk Fe content is constant during serpentinization, we estimate that the contribution of “brown serpentine” in H₂ generation was as large as that of magnetite. Total H₂ produced by complete hydration of olivine 1kg is estimated to be 9.6L (the contribution of “brown serpentine” is 4.5L), which is equivalent to the amount of H₂ dissolved in 54kg of the Kairei hydrothermal fluid (8 mM H₂). Conversion of Fe³⁺-serpentine to Fe-poor serpentine + magnetite at shallower parts may cause a minor absorption of H₂ although we do not have sufficient data to quantify it. The maximum estimation of this study implies a high water/rock ratio in hydrothermal system beneath CIR.

Keywords: Mid-oceanic ridge, hydrothermal field, serpentinite, ferric iron, hydrogen

Lithosphere-Asthenosphere boundary beneath NW Pacific Ocean detected with seismic waveform data

ABE, Yuki^{1*} ; KAWAKATSU, Hitoshi¹ ; SHIOBARA, Hajime¹ ; ISSE, Takehi¹ ; SUGIOKA, Hiroko² ; ITO, Aki² ;
UTADA, Hisashi¹

¹Earthquake Research Institute, The University of Tokyo, ²Japan Agency for Marine-Earth Science and Technology

We have conducted seismic observation around the Shatsky Rise in the northwest Pacific Ocean at 18 stations equipped with a broadband ocean bottom seismometer (BBOBS) for understanding the structure of the Earth's interior and the mechanism of plate motion (Normal Mantle Project). It is important to estimate the upper mantle structure beneath these stations, for revealing existence of partial melt and water in the oceanic upper mantle.

We calculated P-wave and S-wave receiver functions (PRF, SRF) with waveform data obtained from the BBOBSs. We analyzed teleseismic events occurring between June 2010 and September 2014, whose magnitudes are over 5.5. Epicentral distances of the events used for calculating PRF are between 30° and 90°, and those for calculating SRF are between 55° and 90°. Careful handling is required for the data obtained at stations northwest side of the Shatsky Rise because the data are largely affected by reverberations in the thick sediments (Abe and Kawakatsu, 2014, SSJ Fall Meeting). We eliminated frequency components higher than 0.1 Hz from SRF with a Gaussian filter because noise level of the observed waveforms in the frequency domain around 0.2 Hz is high. Frequency components higher than 0.05 Hz were eliminated from PRF for preventing contamination by reverberations in the sediments. We averaged PRFs and SRFs for each station, and obtained a broad negative peak on averaged PRFs and a broad positive peak on averaged SRFs, between 5 s and 10 s. Both these peaks correspond to velocity decrease with depth in the upper mantle. We synthesized PRF and SRF with a model, which contains a discontinuity at depths between 30 km and 150 km, where velocity decreases between 0% and 20% with depth, and searched a model that explains both PRF and SRF obtained at each station. From the search, a model with 8% drop in velocity at 85 km in depth and a model with 4% drop in velocity at 125 km in depth explain the data observed at the northwest and southeast side of the Shatsky Rise the best, respectively. Kawakatsu et al. (2009 Science) detected a discontinuity with downward decreasing velocity at 80 km in depth by an RF analysis of waveform data from borehole BBOBS on north side of Shatsky Rise, and they interpreted the discontinuity as the Lithosphere-Asthenosphere boundary (LAB). The discontinuity detected in this study may also correspond to LAB. The structure of the oceanic crust and sediments and water depth of a station may affect the waveform of RFs. Therefore, we now check how correctly we can constrain the depth and the drop in velocity with different assumptions of the shallower structure.

Keywords: oceanic plate, receiver function, Northwest Pacific Ocean, Lithosphere-Asthenosphere boundary

Sharp gravity increase following an outer-rise earthquake: possibility of viscoelastic rebound by melt-rich channel

MATSUO, Koji^{1*} ; FUKUDA, Yoichi¹ ; TANAKA, Yoshiyuki²

¹Kyoto University, ²The University of Tokyo

We are going to talk about postseismic gravity increase by outer-rise earthquakes, and explain their geophysical mechanism through viscoelastic theory.

Keywords: outer-rise earthquake, melt-rich channel, viscoelastic rebound, GRACE, postseismic gravity change

Earthquake induced deposits during the 2004 off Kii Peninsula earthquakes at a terminal basin

ASHI, Juichiro^{1*} ; OMURA, Akiko¹ ; OKUTSU, Natsumi¹ ; YAMAGUCHI, Asuka¹ ; IRINO, Tomohisa² ; MURAYAMA, Masafumi³ ; IKEHARA, Ken⁴ ; NAKAMURA, Yasuyuki⁵

¹The University of Tokyo, ²Hokkaido University, ³Kochi University, ⁴AIST, ⁵JAMSTEC

Submarine paleoseismology has been advanced mainly by investigation of distribution and age of seismogenic turbidite deposits. However, we have to pay attention to the following issues for the usage of this method. 1) Turbidity currents are also triggered by flood, wave, rapid sedimentation and so on. 2) It is hard to determine a seismic source region by investigation of turbidites originated from more than one sediment-provenance. 3) Turbidity current does not provide sedimentary record or remove the former sequence in some cases. In order to avoid these problems, a terminal basin with a limited small provenance area and without direct river input is an appropriate target. The term "a terminal basin" is a sedimentary depression surrounded by topographic heights that capture all sediments supplied from outside.

The sedimentary basin located between the Kumano forarc basin and the outerarc high corresponds to a terminal basin 250 meter deeper than the surroundings. The core sample collected by R/V Shinsei-maru KS-14-08 from this basin includes thin very fine-grained sand at 17 cm below seafloor and mud with silty clay laminae above it. The surface 17 cm thick mud layer is interpreted to be younger than 1950 because Cesium-137 measurements show constant high value above 17 cm and lower value than detection limit below it. Moreover, excess Pb-210 values show constant high above 17 cm and rapid decrease downward below it. This indicates a sedimentation event for a short period of time. Because the sampling site is isolated from river flood sedimentation area, earthquake shaking is the most plausible trigger of sediment gravity flow. The 2004 off the Kii peninsula earthquakes is a potential candidate within the historical earthquakes in this area after 1950.

Sidescan sonar WADATSUMI survey was conducted in this area in December 2004 just after the Kii peninsula earthquakes. The sidescan sonar image at the terminal basin shows extremely low backscattering intensity suggesting surface veneer of very high water content mud derived from earthquake triggered turbidity flow.

Keywords: turbidite, turbidity current, sedimentary basin, accretionary prism, submarine landslide

Microstructure analysis of earthquake-induced deposits associated with the 2004 off Kii Peninsula earthquakes

OKUTSU, Natsumi^{1*} ; ASHI, Juichiro¹ ; OMURA, Akiko¹ ; YAMAGUCHI, Asuka¹ ; SUGANUMA, Yusuke² ; MURAYAMA, Masafumi³

¹Atmosphere and Ocean Research Institute, The University of Tokyo, ²National institute of Polar Research, ³Center for Advanced Marine Core Research , Kochi University

An ENE-WSW elongated depression is located between the southern margin of the forearc basin and the outer ridge off Kuroshio and a terminal basin that captures all sediments supplied from outside is developed in it. No sediment is supplied from the rivers to this basin, so it is an adequate site to study paleoseismology using seismogenic turbidites.

The result of the Cs-137 and Pb-210 measurements indicates that the upper 17-cm mud layer was deposited immediately after the 2004 off Kii Peninsula earthquakes (Ashi and others, in this Session). We herein investigate the characteristics of the earthquake-induced deposits based on several measurements including their compositions, grain sizes, X-ray CT images, and anisotropy of magnetic susceptibility (AMS).

We observed a very thin fine-grained sand layer of 6 mm thick at 17 cm below seafloor and a massive mud below it on the core split section. On the other hand, the X-ray CT image shows seven silty clay laminations thinning upwards at 6 -15 cm below seafloor, and homogeneous clayey silt above it. The AMS parameters decrease upwards in the interval showing parallel/cross laminations and the lowest value is measured in the overlying silt layer, whereas grain sizes have no significant change. These results indicate that the upper 17 cm layer beginning from the very fine-grained sand can be interpreted to be formed by a low-density sediment gravity flow. Below the depth of 17 cm, the deposition is mainly composed of muddy sediments with a wood chip-enriched thin bed and a very fine-grained thin sand layer at the depth of 32 cm. Structural observations by X-ray CT scanner reveal characteristic structures yielding various orientation oblique to bedding plane at the mud layer 17 cm below seafloor, suggesting that the structure is likely formed by coseismic deformation accompanied by the earthquake in 2004 or earlier ones. Magnetic fabrics derived from AMS measurements and the structure observed by X-ray CT scanner also agree to this picture.

Keywords: turbidity current, anisotropy of magnetic susceptibility, X-ray CT, event deposit

Application of C-14 dating on *Calyptogena* shells for historical fault activity analysis off Tokai, Nankai Trough

YAGASAKI, Kazuhiro^{1*} ; KURAMOTO, Shin'ichi² ; ASHI, Juichiro¹ ; YOKOYAMA, Yusuke¹ ; MIYAIRI, Yosuke¹

¹Atmosphere and Ocean Research Institute, UTokyo, ²Center for Deep Earth Exploration, JAMSTEC

Cold seeps are frequently found at tectonically active continental margins including areas such as the Nankai and Tokai regions. The fluid conduits created by the tectonic activities often form cold seeps, releasing hydrocarbon rich fluids such as methane. Substances such as this are essential for supporting *Calyptogena* bivalve communities to survive through a symbiotic process with the chemosynthetic bacteria. The lifespan of bivalves can be ephemeral due to the conduits altering from tectonic events of converging plate margins, or the source of the hydrocarbon depleting over time. These characteristics may suggest that the *Calyptogena* bivalve shells may hold important information on historical fault activities of the area.

Marine samples originating from the deep sea have often been difficult to radiocarbon date due to the complicated calibration processes involved. Deep circulating ocean currents and sub seafloor seepage of hydrocarbons are main factors responsible for the necessary complex calibration calculations, referred to as the dead carbon effect. DSV *Shinkai* 2000 discovered an unusually large *Calyptogena* bivalve colony in 1997, ranging approximately 200m² off the Daini Tenryu Knoll off Tokai in Japan. Bivalve colonies found are composed mainly of dead shells with few spots of living communities remaining. Past tectonic events may have influenced the methane hydrate layer below to destabilise, releasing significant amounts of methane fluid and gas to the seafloor, consequently allowing bivalves to flourish (Kuramoto, 2001; Ashi et al., 2002; Otsuka et al., 2010).

Amino acid racemisation dating technique was employed on the same shells by Misawa (2004) revealing two different age groups of 0~500 years (white shells) and 1000~2000 years (brown shells), yet the technique was prone to temperature and pH change. This study therefore proposes a novel application of radiocarbon dating of such bivalves to further understand the interaction between local active faults and the bivalve community. Current ¹⁴C age measured range between 1868~1949 year cal AD, coinciding with the 1854 Ansei Tokai earthquake (M8.4). Seafloor mapping, seawater analysis and EPMA and SEM structural analysis of shells from ROV *HyperDolphin* Dives 1355 and 1377 during NT14-07 and NT02-08 respectively, will also be reported.

Keywords: Radiocarbon dating, Cold seep, *Calyptogena* shell, Active fault, Methane

Distribution of methane hydrate BSRs and shallow thermal structure in the Nankai subduction zone

OHDE, Akihiro^{1*} ; OTSUKA, Hironori¹ ; KIOKA, Arata¹ ; ASHI, Juichiro¹

¹Atmosphere and Ocean Research Institute, The University of Tokyo

Thermal structure in subduction zones influences pore pressure and diagenesis such as consolidation, dewatering, cementation, and constrains physical properties of fault-slip plane. Methane hydrate is a clathrate that consists of water and methane. Recently, it attracts attentions not only for marine resources but also for estimates of thermal information below the seafloor using the characteristics of its stabilization under low-temperature and high-pressure conditions. Precise two-dimensional thermal structure ranging from the seafloor to BSR depths is calculated taking topographic effect into account, because subsurface heat flow is affected by bathymetry features.

Geothermal gradients in rougher topography tend to be widely different from that in flat seabeds. To remove this effect, I evaluated the effect by conducting the simple two-dimensional thermal calculation of Blackwell et al. (1980). Additionally, I calculate the Base of Gas Hydrate Stability zone (BGHS) taking into consideration the thermal structure coupled with the topographic effect.

A deepening trend of BSR depths landward of trough floor is confirmed as suggested in previous studies. This observation yields countertrend because the BSR depth should be deepest in the trough floor as methane hydrate is stable under low-temperature and high-pressure conditions. Thus, observed BSR depths suggest that heat flow actually decreases landward of the trough floor.

The investigated BSR depths are constrained from deep heat flux, and vary basically landward of the trough floor. But, in this study, BSR depths are deeper around anticline parts and shallower around syncline. Theoretically, the convex-upward seabed is subject to cooling owing to cold bottom seawater, while the convex-downward one is less subject to the cooling. Evaluations of this kind of topographic effect suggest that syncline can be explained by only the topographic effect. Thus, thermal regime calculated from BSR depths does not change in syncline or slope areas.

In this study, the BSR was confirmed for the first time at the prism toe. The detailed BSR distribution map can contribute to disaster prevention because BSRs have potential to be fault-slip planes. In the Nankai area, geothermal gradient values scatter, but the values can be explained by considering subducting plate age, topographic effect, and sedimentation or erosion. In addition, while distances from seafloor to BSR depths are different even under the same water pressure, the calculation taking topographic effect into account revealed to be able to explain these depth changes. Moreover, the calculated thermal structure over BSR depths considering topographic effect seems to be accurate, because estimated BGHS depths and BSR depths fit well together. Understanding precise BSR depths enables to precisely estimate deposited amount of methane hydrate. This study provides thermal information essential for seismic simulations in subduction zones and for laboratory experiments as analogues to seismic ruptures in plate boundary faults.

Keywords: Nankai subduction zone, methane hydrate BSRs, shallow thermal structure

Physical property of sea bottom surface estimated from fin whale vocalization

IWASE, Ryoichi^{1*}

¹JAMSTEC / CREST, JST

At the cabled observatory off Kushiro-Tokachi in Hokkaido, fin whale vocalizations, which have the frequency range of 15-20 Hz and the duration of about 1 second, were sometimes observed not only with hydrophones but also with ocean bottom seismometers (OBSs) mainly in winter seasons. By using the waveform data of both hydrophone and OBS at OBS1 at the observatory observed from 13:44 to 14:59 JST on December 10th in 2004, the location of the fin whale was estimated. The localization was done based on the incident orientation which was estimated from the horizontal particle motion observed with the OBS and the horizontal range between the OBS and the whale estimated from the time difference of multi-path arrival (TDOMA) in sound pressure data of a hydrophone which includes the reflection at both seafloor and sea surface. During the above observation period, 62 vocalizations were used, whose direct and multi-path arrivals were both identified. The waveforms were band-pass filtered between 10 and 25 Hz and the incident orientation of the particle motion was estimated by applying principal component analysis and by obtaining eigen vector of first main component. As a result it was found that the whale was moving south-south-east near the east of OBS1.

In the previous study carried out in the northeast Atlantic (Harris et al., 2013), the incident angle which was estimated from the apparent emergent angle in the sediments observed with the OBS was used instead of the TDOMA for the localization of the whale. However, the apparent emergent angle is affected by the density and P-wave (pressure wave) velocity of both sediments and water, and is also affected by SV-wave (share wave) velocity of the sediments, which are mostly unknown. This time, the author compared the apparent emergent angle in the sediments observed with the OBS with the incident angle estimated from the TDOMA in order to examine the consistency of those estimations. As a result, good correlation between the apparent emergent angle and the incident angle was confirmed, and the critical incident angle of pressure wave in seawater was estimated to be 60 degrees. Accordingly, the P-wave velocity in sediments was estimated to be about 1.7 km/s according to Snell's law, assuming that sound velocity in water was 1.5 km/s and SV-wave velocity in sediments was very slow.

Keywords: fin whale vocalization, incident angle, apparent emergent angle, critical angle, seismometer, hydrophone

Crustal density structure derived from gravity modelling using results of seismic crustal structure surveys

FUJIOKA, Yukari^{1*} ; ISHIHARA, Takemi²

¹Japan Coast Guard, ²National Institute of Advanced Science and Technology

The Japan Coast Guard (JCG) has conducted marine gravity surveys in Japan's adjacent seas as part of collecting marine-related information to the development and use of the oceans, and possesses enormous amount of marine gravity data. We calculated crustal thickness distribution in the Western Pacific area by applying the gravity inversion method (Ishihara and Koda, 2007) using these data.

Free air anomalies obtained from the satellite altimetry (Sandwell et. al., 2014) were used as a reference in order to correct deviations of marine gravity values of each surveys. In the long wavelength components, gravity data observed and these from the satellite altimetry match well. In the short wavelength components, maritime gravity data were used in preference because gravity data from the satellite altimetry include a few mGal of noises with wavelength of 20-30 km.

The initial density structure model consists of five layers; sea water, sediments, upper crust, lower crust and mantle. The depths of layers of the initial model reflect results of JCG's seismic crustal structure surveys: the depth of basement as boundary between sediments and upper crust is made by interpolation of the depth of the strong reflectors in the reflection cross section obtained from multichannel seismic reflection surveys, and the depths of the top of the lower crust and the Moho are made by interpolation of the depth of area whose velocity gradient of seismic velocity structure cross section obtained from seismic refraction surveys, respectively.

The differences of the observed free air anomalies from the gravity anomalies obtained by model calculation for the initial five layer model were divided into some components by their wavelengths because they include the effects due to the structure such as inhomogeneity in the mantle. The depths of the top of the lower crust and the Moho were obtained by inversion calculation using their anomaly contributions, then the crustal thickness distribution was estimated. According to the results, most of large seamounts are associated with the Moho convex downward, however, some of them have almost no Moho lows below them.

Keywords: gravity, inversion calculation

Seafloor crustal deformation at the Kumano Basin and along the Nankai Trough

TADOKORO, Keiichi^{1*}; FUJII, Cosmo¹; YASUDA, Kenji¹; IKUTA, Ryoya²; UEMURA, Yuichi¹; MATSUHIRO, Kenjiro¹

¹Nagoya University, ²Shizuoka University

Our research group performs monitoring of sea-floor crustal deformation with the GPS/acoustic system at four sites (KMN, KMC, KMS, and KME) on the Kumano Basin. We have already measured 16, 6, 20, and 10 times at KMN (from 2005), KMC (from 2012), KMS (from 2004), and KME (from 2008) sites, respectively. The battery at KME site ran out in the previous year, and we cannot continue to measure at the site. The research vessel we used is Asama of Mie Prefecture Fisheries Research Institute.

We carried out correction of travel-times of acoustic ranging wave and removal of incorrect results of KGPS positioning and ship's attitude measurement before the benchmark position analysis for improving data quality before deriving site velocities. We also fix a correction parameter, related to the relative position of GPS antenna and transducer, at an averaged value for the benchmark position (weight center) determination.

We obtained the horizontal site velocities from linear trends of the time series of benchmark position through the robust estimation method (Tukey's Biweight estimation), adopting REVEL model for the plate motion. The steady horizontal site velocities with relative to the Amurian Plate are: 45 ± 2 mm/yr in N78 \pm 5W direction (KMN), 46 ± 5 mm/yr in N75 \pm 4W (KMS), and 32 ± 12 mm/yr in N69 \pm 21W (KME). These results show no significant difference in the site velocities at the three sites. We installed two different benchmarks on the same weight center position at KMS site. The horizontal site velocity of the other set of benchmark has no significant difference compared to the above-mentioned one at KMS site, which shows high precision of our system.

During the 2011 Tohoku earthquake, it is estimated that the large slip of 40-50 m on the plate interface immediately adjacent to the trench axis. It is, therefore, essential to measure the slip deficit also at the same region along the Nankai Trough. For this reason, we installed a new site, TCA and TOA, on the seafloor 15 and 35 km from the trough axis, respectively. We have already measured four times at the two new sites. A transducer is equipped at the bottom of the research vessels we used, Shinsei Maru and Kaiyo Maru No.3, and we can perform acoustic ranging for distances more than 6,000 m above 5 knot. Now we are carrying out the benchmark position analysis, with checking the effect on the benchmark positioning of sound speed structure in the sea, as well as the data quality of KGPS.

Improvement in the accuracy of GPS/Acoustic measurement using a multi-purpose moored buoy

IMANO, Misae^{1*} ; KIDO, Motoyuki² ; OHTA, Yusaku¹ ; TAKAHASHI, Narumi³ ; FUKUDA, Tatsuya³ ; OCHI, Hiroshi³ ; HINO, Ryota²

¹Graduate School of Science, Tohoku University, ²International Research Institute of Disaster Science, ³Japan Agency for Marine-Earth Science and Technology

In 2011 Tohoku-oki earthquake (Mw 9.0), seafloor geodetic observation using GPS/Acoustic measurement revealed that large co-seismic slip occurred along the Japan trench (Kido et al., 2011; Sato et al., 2011). For clarifying the mechanism of plate boundary earthquakes and forecasting Tsunami immediately, it is necessary to monitor seafloor crustal deformation and Tsunami in the source region. DONET and the GPS buoy system monitor Tsunamis in offshore. On the other hand, horizontal seafloor crustal deformation is measured by GPS/Acoustic surveys, which are mainly carried out by campaigns several times a year. Therefore, we cannot obtain information on co-seismic and post-seismic crustal deformations immediately. Considering the above, JAMSTEC, JAXA, Tohoku University have jointly developed a continuous observation system using a moored buoy and have started its sea-trial at Kumano-nada in 2013 and 2014 (Takahashi et al., 2014). In this study, we evaluate the accuracy of the estimate of horizontal seafloor crustal deformation using the data obtained by this system in the 2014 sea-trial. Moreover, we propose an analysis for improving positioning accuracy.

In general, GPS/A survey is carried out near the center of the transponder array, which cancel out the effect of the time-variation of layered sound speed structure. Due to violation in the assumption of layered structure, positioning accuracy of each shot is 20 ~30 cm. By repeating this in a campaign observation half a day, we realize to measure crustal deformation in a few cm order (Spiess et al., 1998). On the other hand, the buoy is moored by slack cable for observation at strong tide and the acoustic ranging is carried out at a point away from the array center. A set of acoustic ranging consists of 11 pings an interval 65 seconds. This cycle repeated once a week. Therefore, it is not possible to cancel the time variation of the speed sound. Based on the above and the fact that our target is detecting of the co-seismic slip associated with massive earthquake just above the source region, we aim that positioning accuracy is 1m order.

In the acoustic ranging, each travel time is obtained by picking up the maximum peak in correlogram between transmitted and received waves. In the current system, only 1ms of correlograms (8bit, sampling frequency: 100 kHz) are sent to land station to save bandwidth in the satellite communication. However, by investigating the raw data recovering after sea-trial, it is revealed that the travel time of multi-path at sea surface is often sent to land station through the process mentioned above. Imano et al. (2014) proposed the new method to pick up the earliest peak of peaks in a correlogram for a single acoustic signal. We estimate the array center based on Kido et al. (2006) using the travel time obtained by the conventional method and the travel time obtained by Imano et al. (2014). The standard deviation of the estimated array center using the travel time obtained by the conventional method is 3.7 m (East-West component) and 2.6 m (North-South component) in the data in a week, 5.2 m (E-W) and 3.9 m (N-S) in the data in the entire period. On the other hand, the standard deviation using the travel time obtained by Imano et al. (2014) is 0.45 m (East-West component) and 0.34 m (North-South component) in the data in a week, 3.6 m (E-W) and 2.2 m (N-S) in the entire period. The apparent fluctuation of the estimated array center of the latter is smaller than that of the former, in the same week data in particular. However, the fluctuation of the array center is a few meter order in the entire observation period. Therefore, we should take measures such as re-analyzing after determining the position of each transponder in the accuracy about 10 cm in order to aim that the accuracy of GPS/A measurement using the buoy system is 1 m order in the future. In this presentation, we demonstrate and discuss how much the accuracy is improved after the measure.

Keywords: Seafloor crustal deformation, Moored buoy

GANSEKI: Utilize fieldwork information for studying JAMSTEC rock samples

TOMIYAMA, Takayuki^{1*} ; SOMA, Shinsuke² ; HORIKAWA, Hiroki¹

¹JAMSTEC, ²Marine Works Japan, Ltd.

Japan Agency for Marine-Earth Science and Technology (JAMSTEC) carries out several tens to more than a hundred of observation cruises each year, using research vessels e.g. "Mirai," "Kairei," "Kaiyo," "Yokosuka," and "Natsushima". Activities during each cruise differ depending on individual research projects, and more than ten of these cruises involve rock collecting activities. Rock samples are recovered using deep-sea submersibles such as "Shinkai 6500", "Hyper-Dolphin", "Kaiko 7000II" and "Deep Tow", and dredgers. These activities yield tens to more than a hundred of rock samples each year.

JAMSTEC considers its rock sample collection as a common property of human community [1], which can be a resource for research and education of earth-ocean sciences. After up to 2 years of moratorium period during which only on-board researchers can access to samples, JAMSTEC makes the rock samples accessible to second-hand users with research/educational purposes. The information of JAMSTEC rock samples is published through the "GANSEKI" database [2]. Using GANSEKI, users can access to the various information such as basic information (metadata) of 20,663 sampling activities, archive information (inventory data) of 12,243 physical samples, geochemistry data of 19,508 analyses, thin-section photos, publication, and links for associated databases. JAMSTEC rock sample collection includes not only relatively new samples, which were collected after the establishment of curatorial handling in 2008, but also old samples from '80s or '90s, which were donated by researchers.

After the major update of GANSEKI in 2013, which improved the searchability and visibility of user interfaces, the curatorial team has been maintaining inter-database network around GANSEKI. In addition to the cruise and dive information in the DARWIN database[3], GANSEKI users can now access to the abundant field information such as sampling processes, geological and geometrical information, which can be recognized through watching dive photos/movies in the "J-EDI" database [4] and tracing 3D dive tracks on the "JDIVES" data viewer [5]. It is not easy even for experienced researchers to organize and utilize huge data obtained during individual cruises or dives. The inter-database networking among GANSEKI and associated databases are advantageous not only for second-hand users, but also for on-board researchers themselves.

References: [1] "Basic Policies on the Handling of Data and Samples" http://www.jamstec.go.jp/e/database/data_policy.html. [2] "Geochemistry and Archives of Ocean Floor Rocks on Networks for Solid Earth Knowledge Information (GANSEKI)" <http://www.godac.jamstec.go.jp/ganseki/e>. [3] "Data Research System for Whole Cruise Information in JAMSTEC (DARWIN)" <http://www.godac.jamstec.go.jp/darwin/e>. [4] "JAMSTEC E-library of Deep-sea Images (J-EDI)" <http://www.godac.jamstec.go.jp/jedi/e>. [5] "JAMSTEC deep-sea Data-Image Virtual Exploration System (JDIVES)" <http://www.godac.jamstec.go.jp/jdives/e>.

Keywords: marine geology, rock sample, curation, database